American Journal of Pathology, Vol. 165, No. 6, December 2004

Tumorigenesis and Neoplastic Progression

Minodronate, a Newly Developed Nitrogen-Containing Bisphosphonate, Suppresses Melanoma Growth and Improves Survival in Nude Mice by Blocking Vascular Endothelial Growth Factor Signaling

Sho-ichi Yamagishi,* Riichiro Abe,† Yosuke Inagaki,* Kazuo Nakamura,* Hiroshi Sugawara,† Daisuke Inokuma,† Hideki Nakamura,† Tadamichi Shimizu,† Masayoshi Takeuchi,‡ Akihiko Yoshimura,§ Richard Bucala,¶ Hiroshi Shimizu,† and Tsutomu Imaizumi*

From the Department of Internal Medicine III, Kurume University School of Medicine, Kurume, Japan; the Department of Dermatology,† Hokkaido University School of Medicine, Sapporo, Japan; the Department of Biochemistry,‡ Hokuriku University, Kanazawa, Japan; the Division of Molecular and Cellular Immunology,§ Medical Institute of Bioregulation, Kyushu University, Fukuoka, Japan; and the Departments of Medicine and Pathology,¶ Yale University School of Medicine, New Haven, Connecticut*

Angiogenesis, a process by which new vascular networks are formed from pre-existing capillaries, is required for tumors to grow, invade, and metastasize. Vascular endothelial growth factor (VEGF), a specific mitogen to endothelial cells, is a crucial factor for tumor angiogenesis. In this study, we investigated whether minodronate, a newly developed nitrogen-containing bisphosphonate, could inhibit melanoma growth and improve survival in nude mice by suppressing the VEGF signaling. We found here that minodronate inhibited melanoma growth and improved survival in nude mice by suppressing the tumor-associated angiogenesis and macrophage infiltration. Minodronate completely inhibited the VEGF-induced increase in DNA synthesis and tube formation in endothelial cells by suppressing NADPH oxidase-mediated reactive oxygen species generation and Ras activation. Furthermore, minodronate inhibited the VEGF-induced expression of intercellular adhesion molecule-1 and monocyte chemoattractant protein-1 in endothelial cells. Minodronate decreased DNA synthesis and increased apoptotic cell death of cultured melanoma cells as well. Our present study suggests that minodronate might suppress melanoma growth and improve survival in nude mice by two independent mechanisms; one is by blocking the VEGF signaling in endothelial cells, and the other is by inducing apoptotic cell death of melanoma. The present study provides a novel potential therapeutic strategy for the treatment of melanoma. *(Am J Pathol 2004, 165:1865–1874)*

Tumors cannot grow beyond a volume of 1 to 2 mm^3 without establishing a vascular supply because cells must be within 100 to 200 μm of a blood vessel to survive.[1,2] A major event in tumor growth and expansion is the angiogenic switch, an alteration in the balance of proangiogenic and anti-angiogenic molecules that leads to tumor neovascularization.[3] Several lines of evidence implicate vascular endothelial growth factor (VEGF) as the key factor involved in angiogenic switch in human tumors.[4] VEGF and its receptors are expressed at high levels in almost all tumors,[4] and administration of antibodies (Abs) directed against VEGF or dominant-negative forms of the VEGF receptor *flk-1* inhibited tumor growth in nude mice.[5,6] Tumor vessels are genetically stable and less likely to accumulate mutations that allow them to develop drug resistance in a rapid manner.[7] Therefore, targeting the VEGF signaling in neovascula-

Supported in part by grants from Venture Research and Development Centers from the Ministry of Education, Culture, Sports, Science, and Technology, Japan (to S.Y.); and by grants-in-aid for scientific research from the Japan Society for the Promotion of Science (to R.A.).

Accepted for publication August 12, 2004.

Address reprint requests to Dr. Sho-ichi Yamagishi, Department of Internal Medicine III, Kurume University School of Medicine, 67 Asahi-machi, Kurume 830-0011, Japan. E-mail: shoichi@med.kurume-u.ac.jp.

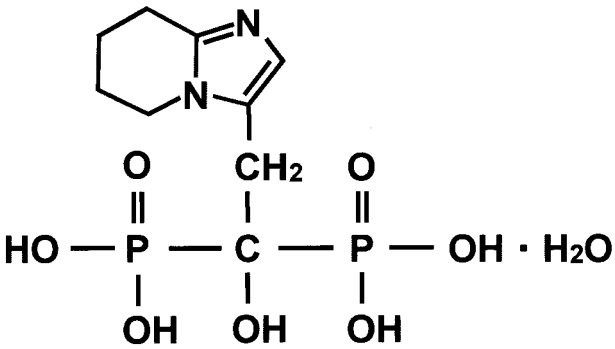

Figure 1. Chemical structure of minodronate. Molecular weight is 340.16.

tures that support tumor growth is considered to be a promising approach to anti-tumor therapy.

Bisphosphonates are potent inhibitors of bone resorption and are widely used drugs for treatment of osteoporosis and osteolytic bone metastasis.[8] *In vitro* anti-tumor properties of bisphosphonates include inhibition of tumor proliferation and invasion and induction of apoptosis of various cancer cell lines.[9,10] Recently, farnesyl pyrophosphate (FPP) synthase has been shown as a molecular target of nitrogen-containing bisphosphonates, and inhibition of posttranslational prenylation of small molecular weight G proteins is likely involved in their anti-resorptive activity on osteoclasts.[11] Bisphosphonates have been reported to accumulate in human vessels.[12] Furthermore, nitrogen-containing bisphosphonates such as ibandronate and zoledronic acid have been shown to inhibit angiogenesis *in vitro*.[13] These observations suggest that nitrogen-containing bisphosphonates might have pleiotropic properties on endothelial cells (ECs) by blocking isoprenoid intermediates, which serve as lipid attachments for a variety of intracellular signaling molecules.[14]

NADPH oxidase activity is required for the angiogenic signaling of VEGF,[15] and small G protein Rac is a critical component of the endothelial NADPH oxidase complex.[16] Further, VEGF is a key factor for melanoma angiogenesis and macrophage infiltration, the extent of which being correlated with tumor prognosis.[17,18] These observations led us to examine whether minodronate, a newly developed nitrogen-containing bisphosphonate, could inhibit melanoma growth and improve survival in nude mice by suppressing the tumor-associated angiogenesis and macrophage infiltration *in vivo*. We also investigated in the present study whether and how minodronate could block the VEGF signaling in ECs.

Materials and Methods

Growth of G361 Xenografts in Nude Mice

One million G361 cells were injected intradermally into the upper flank of 6-week-old female athymic nude mice ($n = 5$ in each group). Mice received intraperitoneal injections of 5 μg of minodronate (Yamanouchi Pharmaceutical Co., Tokyo, Japan) or physiological saline solution daily. The chemical structure of minodronate is shown in Figure 1. Its molecular weight is 340.16. The smallest and largest diameters of tumors were measured at 5-day intervals with a digital caliper, and tumor volumes were calculated using the following formula: volume (mm^3) = [(smallest diameter)^2 $\times$ (largest diameter)]/2. All animal procedures were conducted according to the guidelines provided by the Hokkaido University Institutional Animal Care and Use Committee under an approved protocol.

Immunofluorescence Staining of Tumor Vessels and Macrophages

Five cryostat sections of tumor xenograft were stained with fluorescein isothiocyanate-conjugated rat anti-mouse CD31 or Mac-3 Abs (Becton Dickinson, Franklin Lakes, NJ) as described previously.[19] Nuclei were stained with propidium iodide. Three different fields at $\times$60 magnification were examined on each section with confocal laser-scanning fluorescence microscopy. Green fluorescence-positive area in three different fields of each section was measured.

Assay for in Situ Apoptosis

Sections of tumor xenograft were stained with hematoxylin and eosin for morphological analysis. Terminal dUTP nick-end labeling assay was performed using an *in situ* apoptosis detection kit according to the manufacturer's instructions (Roche Diagnostics GmbH, Mannheim, Germany). The number of apoptotic cells was counted in 10 randomly selected fields at $\times$200 magnification using confocal laser-scanning fluorescence microscopy.

Cell Culture Conditions

The human adult skin microvascular ECs were incubated in endothelial cell basal medium (EBM) medium (Clonetics Corp., San Diego, CA) supplemented with 5% fetal bovine serum and 0.4% bovine brain extracts in the presence or absence of 10 ng/ml VEGF (PeproTech, London, UK), 10 μmol/L (3.4 μg/ml) minodronate, 100 nmol/L diphenylene iodonium (DPI) (Sigma, St. Louis, MO), 1 μg/ml geranylgeranyl pyrophosphate (GGPP) (Sigma), 10 μmol/L FTI-276 (Calbiochem, San Diego, CA), 1 μmol/L GGTI-286 (Calbiochem), 1 mmol/L *N*-acetylcysteine (Sigma), 1 μg/ml monoclonal Abs (mAbs) against human intercellular adhesion molecule-1 (ICAM-1) (R&D Systems, Minneapolis, MN), dominant-negative human Rac-1 mutant (DN-RacT17N), or dominant-negative human Ras mutant (DN-RasS17N). G361 melanoma cells (American Type Culture Collection, Manassas, VA) were incubated in Dulbecco's modified Eagle's medium supplemented with 10% fetal bovine serum and 100 U/ml penicillin/streptomycin in the presence or absence of various concentrations of minodronate or 0.5 μg/ml FPP (Sigma).

Intracellular Reactive Oxygen Species (ROS) Generation

Intracellular ROS generation was detected by using the fluorescent probe CM-H_2DCFDA (Molecular Probes Inc., Eugene, OR) as described previously.[20] Briefly, cells (2×10^4/96-well-plate) were loaded with 10 μmol/L CM-H_2DCFDA, incubated for 45 minutes at 37°C, and analyzed in a Fluoroskan Ascent FL (Thermo Labsystems, Helsinki, Finland) using the Ascent Software for Windows program.

In Situ *ROS Generation in Tumor ECs*

The oxidative fluorescent probe dihydroethidium (Molecular Probes Inc.) was used to detect *in situ* levels of ROS in tumor ECs according to the method of Miller and colleagues.[21] Briefly, the unfixed frozen tissues were cut into 10-μm-thick sections. The sections were stained with fluorescein isothiocyanate-conjugated rat anti-mouse CD31 Abs (Beckton Dickinson) and then with 2 μmol/L dihydroethidium. Three different fields at ×60 magnification were examined on each section with confocal laser-scanning fluorescence microscopy. Red fluorescence-positive area in three different fields of each section was measured.

Transfection of DN-RacT17N and DN-RasS17N

The DN-RacT17N expression vector was kindly provided by Dr. Y. Horiguchi, Department of Bacterial Toxicology, Research Institute for Microbial Diseases, Osaka University, Osaka, Japan. The DN-RasS17N expression vector was kindly provided by Dr. T. Sato, Faculty of Bioscience and Biotechnology, Tokyo Institute of Technology, Tokyo, Japan. ECs were transiently transfected with either DN-RacT17N, DN-RasS17N or an empty vector using Tfx-50 reagent according to the manufacture's instructions (Promega, Madison, WI).

Measurement of [^{3}H]Thymidine Incorporation in ECs

[^{3}H]Thymidine incorporation in cells was determined as described previously.[22]

Assay for Ras Activation

ECs were incubated with or without 10 ng/ml VEGF for 24 hours in the presence or absence of 10 μmol/L minodronate or 100 nmol/L DPI. Ras activity then was measured using a Ras Activation Assay kit (Upstate Biotechnology Inc., Charlottesville, VA) following the manufacturer's instructions.

Assay for in Vitro *Tube Formation*

In vitro tube formation was assayed as described previously.[23] Briefly, wells of 24-well culture cluster dishes (Costar 3524; Costar, Cambridge, MA) were coated with Matrigel solution (250 μl/well; Beckton Dickinson, Bedford, MA), then allowed to solidify for at least 1 hour at 37°C. ECs (4×10^4 cells/well) were then seeded on Matrigel with 10 ng/ml of VEGF in the presence or absence of 10 μmol/L minodronate. After 6 hours, four microscopic fields selected at random were photographed, and the lengths of capillary-like structures were measured. The vessel structures were confirmed by electron microscopic analysis.

Primers and Probes

Primer sequences used in semiquantitative reverse transcriptase-polymerase chain reactions (RT-PCRs) were 5′-AATGGGGCTGGGACTTCTCATTGG-3′ and 5′-GCCTGGGTGACAGAGCGAGAGCTT-3′ for human ICAM-1 mRNA, and 5′-AACTGAAGCTCGCACTCTCG-3′ and 5′-TCAGCACAGATCTCCTTGGC-3′ for human monocyte chemoattractant protein-1 (MCP-1) mRNAs. Sequences of the upstream and downstream primers used in RT-PCR for detecting β-actin mRNAs were the same as described previously.[24]

Semiquantitative RT-PCR

Poly(A)$^+$ RNAs were isolated from cells, and analyzed by RT-PCR as described previously.[25] The amounts of poly(A)$^+$ RNA templates (30 ng) and cycle numbers (33 cycles for ICAM-1 gene; 30 cycle for MCP-1 gene; 22 cycles for β-actin gene) for amplification were chosen in quantitative ranges, in which reactions proceeded linearly, that had been determined by plotting signal intensities as functions of the template amounts and cycle numbers.[25]

Assay of MOLT-3 Cell Adhesion to ECs

Molt-3 cell adhesion to ECs was assayed according to the method of de Clerck and colleagues.[26] Briefly, ECs were treated with 10 ng/ml of VEGF in the presence or absence of 10 μmol/L minodronate or 1 μg/ml ICAM-1 mAbs for 24 hours, and then incubated with BCECF-AM-labeled Molt-3 cells for 30 minutes. After incubation, the cells were solubilized by 1% Triton X-100 and the fluorescent intensities of the cells were measured.

Measurement of MCP-1

MCP-1 proteins released into media were measured with an enzyme-linked immunosorbent assay (ELISA) system according to the manufacturer's instructions (R&D Systems).

Assay for in Vitro *Apoptosis*

G361 cells were incubated with the indicated concentrations of minodronate in the presence or absence of 0.5 μg/ml of FPP for 24 hours. Then the cells were lysed and

the supernatant was analyzed in an ELISA for DNA fragments (Cell Death Detection ELISA; Roche Molecular Biochemicals, Mannheim, Germany) according to the manufacturer's instructions.

Statistical Analysis

All values were presented as means ± SE. Unless otherwise indicated, one-way analysis of variance followed by the Scheffé *F*-test, was performed for statistical comparisons. In Figure 2, A, C, D, and E, and Figure 3C, unpaired *t*-test was performed for comparison between control and minodronate-treated groups; $P < 0.05$ was considered significant.

Results

Minodronate Inhibits Melanoma Growth and Improves Survival in Nude Mice

Because minodronate has been reported to dose dependently reduce osteolytic bone metastases in nude mice at the range of 0.2 to 20 μg/mouse/day,[27] we chose the dose of 5-μg daily injection of minodronate in our animal experiments. We first investigated whether minodronate could inhibit melanoma growth in nude mice. G361 xenograft melanoma cells formed rapidly growing tumors in nude mice, reaching 500 to 600 mm^3 after 40 days. In contrast, intraperitoneal daily injection of 5 μg of minodronate almost completely inhibited the *in vivo* tumor growth of G361 cells throughout an observation period of up to 40 days (Figure 2, A and B).

Tumor-associated angiogenesis and macrophage infiltration have been known to play an important role in tumor growth and expansion *in vivo*.[28,29] So, we next studied the effects of minodronate on angiogenesis and macrophage infiltration in G361 melanoma xenografts. Minodronate treatment was found to significantly inhibit tumor-associated angiogenesis and macrophage infiltration in nude mice (Figure 2, C and D, respectively). These observations suggest that minodronate might inhibit melanoma growth in nude mice by blocking the tumor-associated angiogenesis and macrophage infiltration *in vivo*.

Tumors cannot survive without establishing a vascular supply.[1,2] Histological examinations revealed extensive areas of tumor necrosis in minodronate-treated G361 xenograft (Figure 2E). Furthermore, apoptotic cell death of melanoma xenografts was significantly increased by the treatment of minodronate. The Kaplan-Meier analysis showed that the rate of host mouse survival was significantly higher in minodronate-treated group than that in the control group (Figure 2F). None of the minodronate-treated mice died throughout an observation period of up to 100 days.

Minodronate Inhibits VEGF-Induced ROS Generation in ECs

VEGF is a key factor for tumor angiogenesis and macrophage infiltration, thus being involved in melanoma growth and progression.[17,18,30] Because ROS generation is reported to be required for the VEGF signaling in ECs,[31] we first studied whether minodronate could inhibit the ROS generation elicited by VEGF. After the intraperitoneal administration of 5 μg of minodronate, its peak plasma concentration reaches ~10 μmol/L (unpublished data). Therefore, we did the following *in vitro* experiments with minodronate at the concentration of 10 μmol/L. Minodronate or DPI, an inhibitor of NADPH oxidase, completely inhibited the VEGF-induced ROS production in ECs (Figure 3A). Further, the inhibitory effect of minodronate on ROS generation was completely reversed by GGPP. These results suggest that VEGF induces ROS generation through NADPH oxidase and that minodronate inhibits the ROS generation by suppressing geranylgeranylation of Rac, one of the important components of NADPH oxidase complex.[16] Pharmacological inhibitors are not absolutely specific to one cellular target. Because DPI can inhibit other superoxide generating enzymes, we performed experiments using molecular techniques. Overexpression of DN-RacT17N also prevented the increase of ROS generation in VEGF-exposed ECs (Figure 3B). These observations also indicate that Rac is directly involved in the VEGF-induced ROS production in microvascular ECs. Minodronate treatment was also found to decrease *in situ* ROS generation in tumor ECs (Figure 3C). Thus, minodronate exerts antioxidative effects on ECs of tumor-associated blood vessels probably by blocking the VEGF signaling *in vivo*.

Minodronate Inhibits VEGF-Induced DNA Synthesis and Tube Formation in ECs

We next investigated a functional role of NADPH oxidase-mediated ROS generation in VEGF-induced angiogenesis. DPI or an anti-oxidant, *N*-acetylcysteine, completely inhibited the VEGF-induced increase in DNA synthesis, suggesting that NADPH oxidase-derived ROS is involved in the VEGF signaling to angiogenesis (Figure 4A). Inactivation of Rac by 10 μmol/L minodronate or a geranylgeranyltransferase inhibitor, GGTI-286, or overexpression of DN-RacT17N also prevented the VEGF effect, thus demonstrating that geranylgeranylation of Rac is necessary for the angiogenic signals of VEGF (Figure 4, B and C). However, in contrast to the case with ROS production, the effect of minodronate on DNA synthesis was not reversed by GGPP. These results suggest that inactivation of other G proteins might also be involved in the anti-angiogenic effects of minodronate. Minodronate at lower concentrations (0.1 and 1 μmol/L) did not affect DNA synthesis in ECs, irrespective of the presence or absence of VEGF (data not shown). These findings suggest that, unlike the effects of statins, minodronate does not have biphasic actions on DNA synthesis in ECs at the concentrations of 0.1 to 10 μmol/L.[32] Furthermore, minodronate did not induce apoptotic cell death in ECs exposed to VEGF (data not shown).

We next examined the involvement of Ras in the VEGF signaling to angiogenesis. VEGF was found to activate Ras in microvascular ECs, which was completely pre-

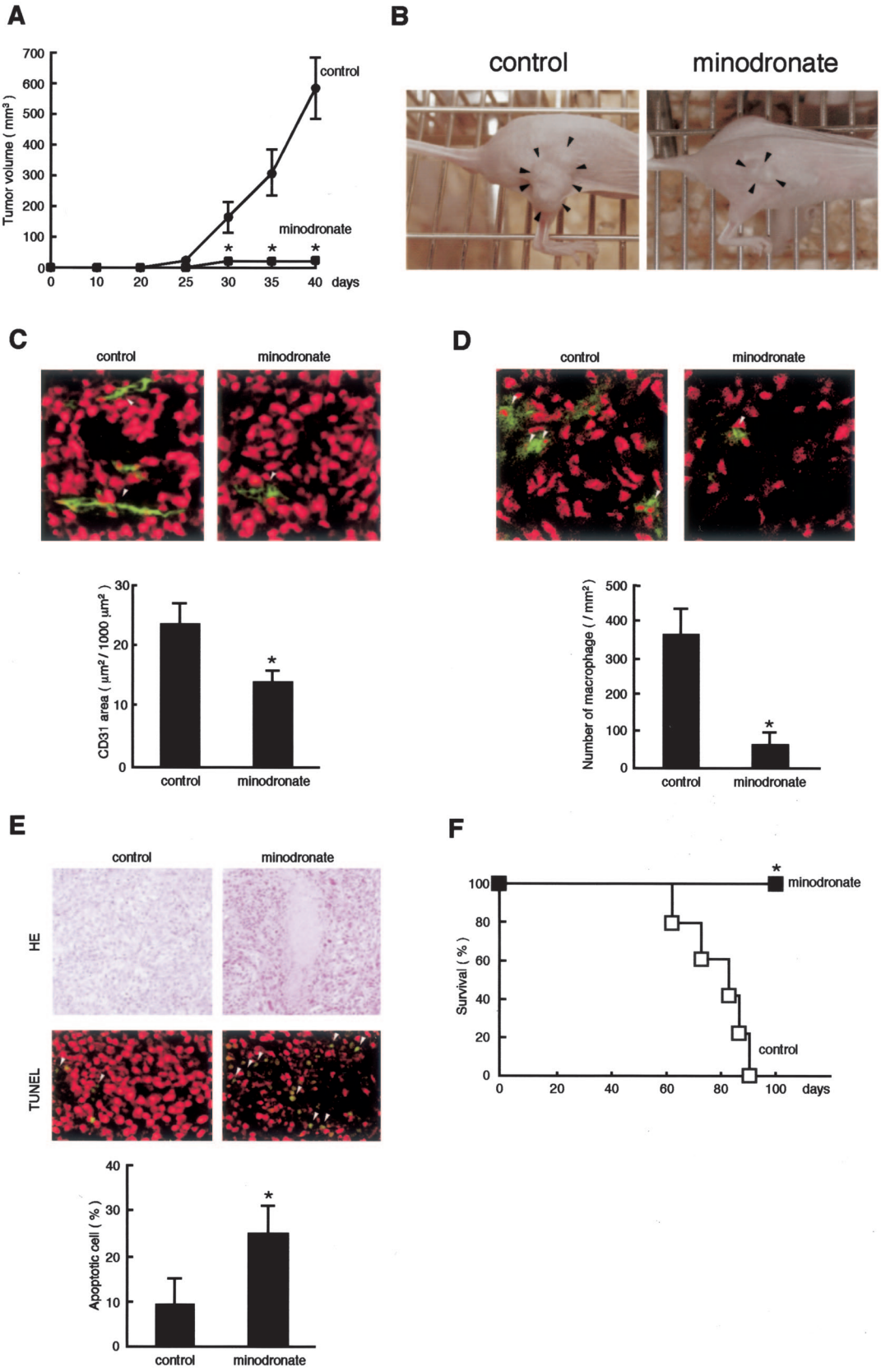

Figure 2. Effects of minodronate on tumor growth (**A** and **B**), angiogenesis (**C**), macrophage infiltration (**D**), apoptosis (**E**), and survival rate (**F**) in nude mice. **A:** Each group (minodronate-treated or nontreated control group) was composed of five athymic nude mice. **B:** Typical photographs were taken after 40 days of injection. **Arrowheads** indicate tumors. **C:** Five cryostat sections of tumor xenograft were stained. Green fluorescence-positive areas in three different fields of each section were measured. **Arrowheads** indicate CD31-positive ECs (green). **D: Arrowheads** indicate Mac-3-positive macrophages (green). **E:** The number of apoptotic cells was counted in 10 randomly selected fields. **Arrowheads** indicate apoptotic cells (green). Tumor nuclei were stained in red. *, $P < 0.01$ compared to control mice. **F:** Kaplan-Meier analysis.

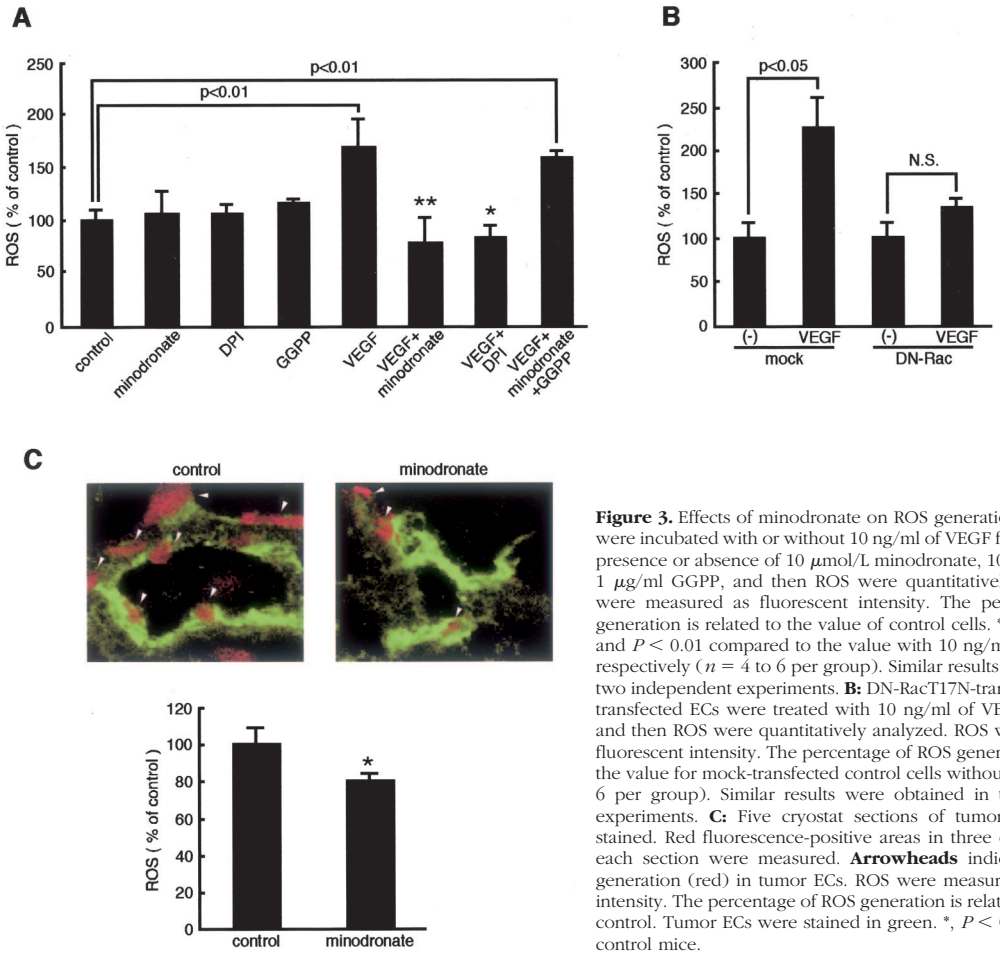

Figure 3. Effects of minodronate on ROS generation in ECs. **A:** ECs were incubated with or without 10 ng/ml of VEGF for 24 hours in the presence or absence of 10 μmol/L minodronate, 100 nmol/L DPI, or 1 μg/ml GGPP, and then ROS were quantitatively analyzed. ROS were measured as fluorescent intensity. The percentage of ROS generation is related to the value of control cells. * and **, $P < 0.05$ and $P < 0.01$ compared to the value with 10 ng/ml of VEGF alone, respectively ($n = 4$ to 6 per group). Similar results were obtained in two independent experiments. **B:** DN-RacT17N-transfected or mock-transfected ECs were treated with 10 ng/ml of VEGF for 24 hours, and then ROS were quantitatively analyzed. ROS were measured as fluorescent intensity. The percentage of ROS generation is related to the value for mock-transfected control cells without VEGF ($n = 4$ to 6 per group). Similar results were obtained in two independent experiments. **C:** Five cryostat sections of tumor xenograft were stained. Red fluorescence-positive areas in three different fields of each section were measured. **Arrowheads** indicate *in situ* ROS generation (red) in tumor ECs. ROS were measured as fluorescent intensity. The percentage of ROS generation is related to the value of control. Tumor ECs were stained in green. *, $P < 0.05$ compared to control mice.

vented by minodronate or DPI (Figure 4D). Further, inactivation of Ras by a farnesyltransferase inhibitor, FTI-276, or overexpression of DN-RasS17N also inhibited the increase in DNA synthesis in VEGF-exposed ECs (Figure 4, E and F). These observations suggest that Ras is a downstream effector of ROS derived form NADPH oxidase and that the anti-angiogenic effects of minodronate can be attributed to inhibition of both Rac and Ras prenylation.

The process of angiogeneis is completed by the formation of microvascular tubes.[23] *In vitro* assays for tube formation of ECs have been developed and used to study this critical step of angiogenesis. Therefore, we further studied the effect of minodronate on tube formation on Matrigel, where ECs take only several hours to associate with each other and to form microtubes.[23] Minodronate completely prevented the VEGF-induced tube formation on Matrigel (Figure 4G). These observations suggest that minodronate could inhibit tube formation of microvascular ECs, the key steps of angiogenesis by blocking the VEGF signaling as well.

Minodronate Inhibits VEGF-Induced ICAM-1 and MCP-1 Overexpression in ECs

VEGF also acts as a proinflammatory cytokine.[33,34] To determine whether minodronate could block the proinflammatory signals of VEGF, we investigated the effects of minodronate on ICAM-1 and MCP-1 expression in VEGF-exposed ECs. Minodronate completely inhibited the VEGF-induced up-regulation of ICAM-1 and MCP-1 mRNA levels in microvascular ECs (Figure 5A). Because our RT-PCR analyses are semiquantitative, to confirm the mRNA findings, we did leukocyte adhesion assay and MCP-1 ELISA. Minodronate inhibited ICAM-1-mediated Molt-3 cell adhesion to, and MCP-1 overproduction in, microvascular ECs (Figure 5, B and C). Cell-based ELISA confirmed that VEGF actually induced ICAM-1 protein expression, which was completely blocked by minodronate (data not shown). GGTI-286 or FTI-276, a geranylgeranyltransferase or farnesyltransferase inhibitor, respectively, also inhibited the VEGF-induced up-regulation of ICAM-1 and MCP-1 (data not shown), suggesting the involvement of both Rac and Ras in the VEGF signaling to inflammation as well.

Minodronate Inhibits DNA Synthesis and Induces Apoptosis in Cultured G361 Melanoma Cells

We next investigated the direct effects of minodronate on DNA synthesis and apoptotic cell death of cultured G361 cells *in vitro*. Minodronate was found to decrease DNA

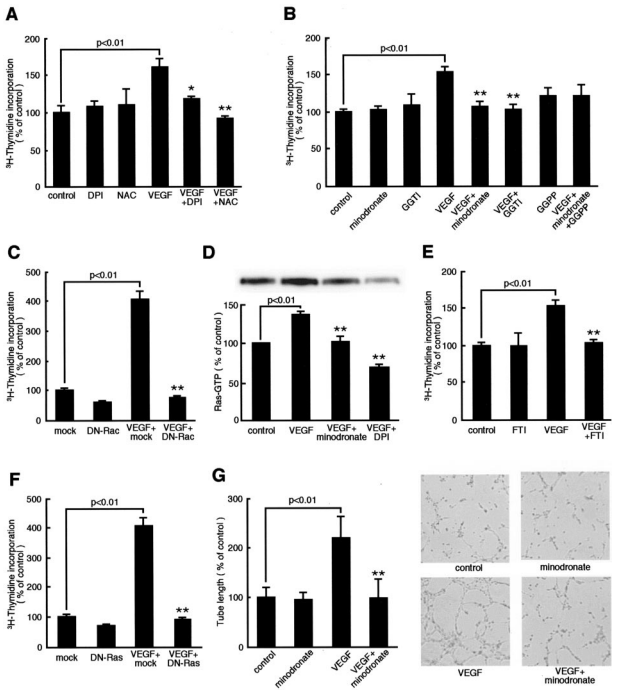

Figure 4. Effects of minodronate on growth and tube formation of microvascular EC. **A**, **B**, and **E:** ECs were incubated with or without 10 ng/ml of VEGF for 24 hours in the presence or absence of 100 nmol/L DPI, 1 mmol/L *N*-acetylcysteine, 10 μmol/L minodronate, 1 μmol/L GGTI-286, 1 μg/ml GGPP, or 10 μmol/L FTI-276, and then [^{3}H]thymidine incorporation was measured. The percentage of [^{3}H]thymidine incorporation is related to the value of the control. One hundred percent indicates 25,743 cpm. **C** and **F:** DN-RacT17N-, DN-RasS17N-, or mock-transfected ECs were treated with 10 ng/ml of VEGF for 24 hours, and then [^{3}H]thymidine incorporation was measured. The percentage of [^{3}H]thymidine incorporation is related to the value of mock-transfected cells without VEGF. One hundred percent indicates 5623 cpm. **D:** Ras activity. ECs were incubated with or without 10 ng/ml of VEGF for 24 hours in the presence or absence of 10 μmol/L minodronate or 100 nmol/L DPI. The percentage of band density is related to the value of the control. **G:** ECs were seeded on Matrigel and incubated with or without 10 ng/ml of VEGF for 6 hours in the presence or absence of 10 μmol/L minodronate. The percentage of length is related to the value of the control. One hundred percent indicates 4.65 mm/mm^2. * and **, $P < 0.05$ and $P < 0.01$ compared to the value with 10 ng/ml of VEGF alone, respectively (n = 4 to 6 per group). Similar results were obtained in two independent experiments.

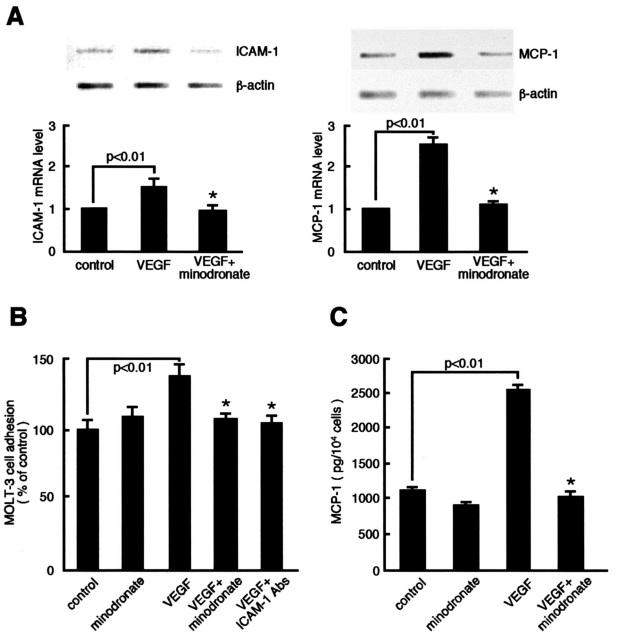

Figure 5. Effects of minodronate on ICAM-1 and MCP-1 expression in VEGF-exposed ECs. **A:** ECs were incubated with or without 10 ng/ml of VEGF for 4 hours in the presence or absence of 10 μmol/L minodronate. Thirty ng of poly(A)$^+$ RNAs were transcribed and amplified by PCR. Each **bottom** panel shows quantitative representation of ICAM-1 and MCP-1 gene induction. Data are normalized by the intensity of β-actin mRNA-derived signals and then related to the value of the control. **B:** ECs were incubated with or without 10 ng/ml of VEGF for 24 hours in the presence or absence of 10 μmol/L minodronate or 1 μg/ml of mAbs against human ICAM-1. Molt-3 cell adhesion was measured as fluorescent intensity. The percentage of Molt-3 cell adhesion is related to the value of control cells. **C:** MCP-1 content in the medium was measured. *, $P < 0.01$ compared to the value with VEGF alone (n = 4 to 6 per group). Similar results were obtained in two independent experiments.

synthesis and increase apoptotic cell death of melanoma cells in a dose-dependent manner (Figure 6, A and B). Minodronate at 10 μmol/L, which effectively blocked the VEGF signaling in cultured ECs, significantly induced apoptotic cell death of melanoma cells, whose effects were completely reversed by the addition of 0.5 μg/ml of FPP (Figure 6C). GGPP at 1 μg/ml did not affect the proapoptotic effects of minodronate *in vitro* (data not shown). These results suggest that minodronate could act on melanoma cells directly to induce apoptosis via suppression of Ras farnesylation.

Discussion

We demonstrated in the present study for the first time that minodronate, a nitrogen-containing bisphosphonate, suppressed melanoma growth and improved survival in nude mice by blocking the tumor-associated angiogenesis and macrophage infiltration. We also found here that minodronate blocked the VEGF signaling to angiogenesis and inflammation in microvascular ECs by suppressing NADPH oxidase-mediated ROS generation and Ras activation. Minodronate has previously been shown to inhibit osteolytic bone metastases of human small-cell lung cancer in natural killer cell-depleted severe combined immunodeficient mice.[35,36] The present study has extended these previous works, thus suggesting that minodronate could be a promising anti-melanoma drug as well.

Several lines of evidence implicate VEGF as the key factor involved in melanoma growth and metastasis.[4] VEGF expression levels are associated with angiogenesis and macrophage infiltration, the extent of which being correlated with melanoma prognosis.[17,18,30] Our present study suggests that minodronate might inhibit melanoma growth and expansion by blocking the VEGF signaling *in vivo*. Figure 7 illustrates a proposed scheme, by which VEGF promotes growth and expansion in melanoma xenografts; VEGF might induce the tumor-associated angiogenesis and macrophage infiltration through NADPH oxidase-mediated ROS generation and Ras activation in ECs. Minodronate could block the VEGF signaling via inhibition of protein prenylation of both Rac and Ras, thus suppressing melanoma growth and subsequently improving survival in nude mice. In our present study, the effects of minodronate on VEGF-induced ROS genera-

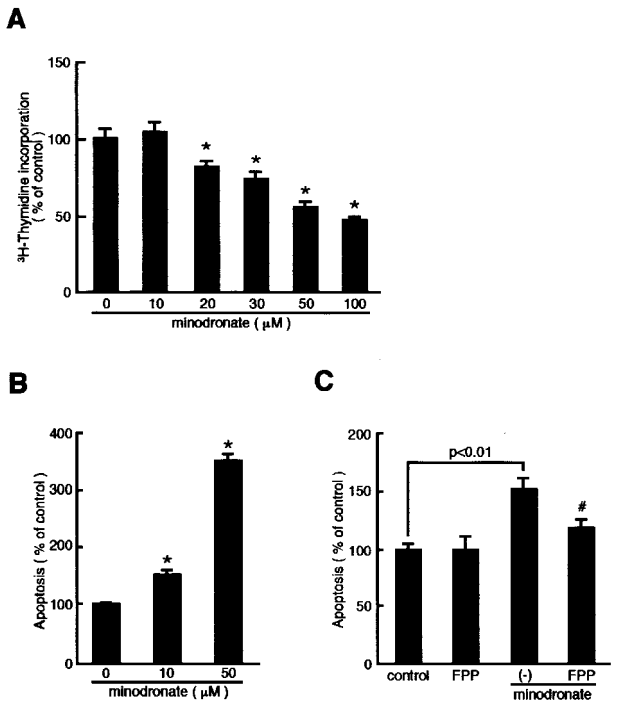

Figure 6. Effects of minodronate on DNA synthesis (**A**) and apoptosis (**B** and **C**) in cultured melanoma cells. G361 melanoma cells were incubated with the indicated concentrations of minodronate in the presence or absence of 0.5 μg/ml of FPP for 24 hours. The percentage of [^{3}H]thymidine incorporation is related to the value of the control. One hundred percent indicates 38,620 cpm. Apoptotic cell death was measured as absorbance at 405 nm. The percentage of apoptotic cell death is related to the value of the control without minodronate. *, $P < 0.01$ compared to the control value. #, $P < 0.01$ compared to the value with 10 μmol/L minodronate alone. $N = 4$ to 6 per group. Similar results were obtained in two independent experiments.

tion, DNA synthesis, and tube formation in cultured ECs were quite strong, whereas those on ROS generation in ECs *in vivo* and tumor angiogenesis were modest. These observations suggest that angiogenic factors other than VEGF could also be involved in tumor angiogenesis in melanoma xenografts.

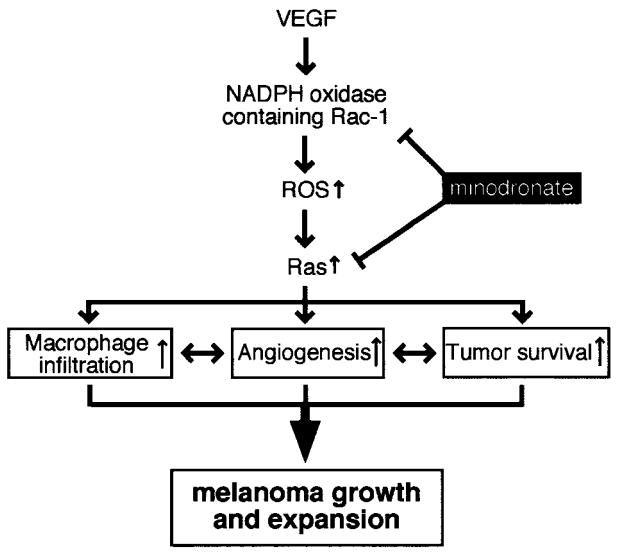

Figure 7. Scheme of possible molecular mechanisms for minodronate-induced growth suppression of melanoma.

It is well known that a number of pathophysiological stimuli induce EC activation as a function of NADPH oxidase-mediated ROS-induced signal transduction.[37] Indeed, NADPH oxidase-derived ROS generation is reported to be required for the angiogenic signaling of VEGF *in vitro*.[15,31] Our present study has extended the previous works. We demonstrated here that geranylgeranylation of Rac, one of the important components of NADPH oxidase, was indispensable for the angiogenic signaling of VEGF and that minodronate blocked the VEGF signaling to angiogenesis by inhibiting NADPH oxidase-mediated ROS generation. Nitrogen-containing bisphosphonates are known to inhibit FPP synthase, thus blocking synthesis of isoprenoid intermediates, FPP and GGPP, which are, respectively, essential for membrane attachment and the biological activity of small G proteins such as Ras and Rac.[11,12,14] These observations suggest that minodronate could block the VEGF signaling in ECs via inhibition of geranylgeranylation of Rac.

In this study, the anti-angiogenic effects of minodronate on VEGF-exposed ECs were not reversed by GGPP. These results suggest that G proteins other than Rac might also be involved in the downstream signaling of VEGF. We obtained the following evidence that Ras was a downstream effector of NADPH oxidase-mediated ROS generation: VEGF activated Ras, which was completely blocked by minodronate or an inhibitor of NADPH oxidase, DPI (Figure 4D); and inactivation of Ras by a farnesyltransferase inhibitor, FTI-276, or overexpression of DN-RasS17N inhibited the angiogenic effects of VEGF on microvascular ECs (Figure 4, E and F). Ras has been proposed as a key regulator of the signaling cascade triggered by oxidative stress,[38–40] and is also required for mitogenic signals of various growth factors including VEGF.[41,42] Taken together, our present study suggests that farnesylation of Ras is also a target of minodronate and that the anti-angiogenic effect of minodronate on VEGF-exposed ECs could be attributed to inhibition of protein prenylation of both Rac and Ras.

VEGF also acts as a proinflammatory cytokine; it not only induces ICAM-1 in ECs, but also stimulates secretion of MCP-1 that recruits leukocytes to sites of inflammation.[33,34] ICAM-1 and MCP-1 are involved in macrophage infiltration into tumors as well, the extent of which is correlated with tumor neovascularization.[43,44] We demonstrated here that minodronate inhibited leukocytes adhesion to VEGF-exposed ECs by suppressing ICAM-1 expression. Further, minodronate inhibited MCP-1 expression both at mRNA and protein levels. Because GGTI-286 or FTI-276, a geranylgeranyltransferase or farnesyltransferase inhibitor, respectively, also inhibited the proinflammatory signals of VEGF (data not shown), minodronate could block the VEGF signaling to inflammation in ECs by inhibiting protein prenylation of both Rac and Ras, as the case in angiogenesis. Although we did not investigate whether minodronate could inhibit peripheral monocyte adhesion to VEGF-exposed ECs, the present study suggests that minodronate could inhibit the tumor-associated macrophage infiltration by suppressing the VEGF signaling to ICAM-1 and MCP-1 overexpression. VEGF has been known to induce expression of ICAM-1

and MCP-1 through the redox-sensitive transcriptional factor, NF-κB activation in ECs.[33,34] Minodronate may inhibit the NF-κB activation induced by VEGF. These observations suggest that the VEGF signaling to inflammation in ECs might also be coupled to the redox state of the cell and that minodronate exerts anti-inflammatory effects on VEGF-exposed ECs through its anti-oxidative properties. Minodronate treatment decreased *in situ* ROS generation in tumor ECs, further supporting our concept that minodronate might block the VEGF signaling *in vivo* through its anti-oxidative properties.

We also found here that minodronate at 10 μmol/L, which effectively blocked the VEGF signaling in cultured ECs, induced apoptotic cell death of cultured G361 cells, whose effects were completely reversed by FPP, but not GGPP (Figure 6C). These results suggest that minodronate acted on melanoma cells directly to induce apoptosis via inhibition of farnesylation of Ras. Essential roles of oncogenic Ras in melanoma genesis and maintenance are reported in mouse models, thus suggesting that proapoptotic effects of minodronate observed in our *in vivo* experiments could be attributed partly to its direct effects on melanoma cells.[45]

Taken together, the present study has highlighted two beneficial aspects of the effects of minodronate on melanoma growth and expansion; one is the suppression of tumor-associated angiogenesis and macrophage infiltration probably by blocking the VEGF signaling *in vivo*, and the other is induction of apoptosis in tumor cells. This scenario could possibly explain why the effects of minodronate on tumor growth and survival were extremely impressive, whereas those on tumor angiogenesis were modest.

Our present study provides a novel potential therapeutic efficacy of minodronate for the treatment of melanoma. We do not know whether the other types of nitrogen-containing bisphosphonates have the same anti-tumor effects on melanoma xenografts. Clinical investigation is needed to evaluate the efficacy of this new pharmacological approach as an anti-tumor therapy.

References

1. Holmgren L, O'Reilly MS, Folkman J: Dormancy of micrometastases: balanced proliferation and apoptosis in the presence of angiogenesis suppression. Nat Med 1995, 1:149–153
2. Carmeliet P, Jain RK: Angiogenesis in cancer and other diseases. Nature 2000, 407:249–257
3. Fidler IJ, Ellis LM: The implications of angiogenesis for the biology and therapy of cancer metastasis. Cell 1994, 79:185–188
4. Senger DR, van de Water L, Brown LF, Nagy JA, Yeo KT, Yeo TK, Berse B, Jackman RW, Dvorak AM, Dvorak HF: Vascular permeability factor in tumor biology. Cancer Metastasis Rev 1993, 12:303–324
5. Kim KJ, Li B, Winer J, Armanini M, Gillett N, Phillips HS, Ferrara N: Inhibition of vascular endothelial growth factor-induced angiogenesis suppresses tumor growth in vivo. Nature 1993, 362:841–844
6. Millauer B, Shawve LK, Plate KH, Risau W, Ullrich A: Glioblastoma growth inhibited in vivo by a dominant-negative Flk-1 mutant. Nature 1994, 367:576–579
7. Scappaticci FA: Mechanisms and future directions for angiogenesis-based cancer therapies. J Clin Oncol 2002, 20:3906–3927
8. Brown DL, Robbins R: Developments in the therapeutic applications of bisphosphonates. J Clin Pharmacol 1999, 39:651–660
9. Green JR, Clezardin P: Mechanisms of bisphosphonate effects on osteoclasts, tumor cell growth, and metastasis. Am J Clin Oncol 2002, 25:S3–S9
10. Clezardin P, Fournier P, Boissier S, Peyruchaud O: In vitro and in vivo antitumor effects of bisphosphonates. Curr Med Chem 2003, 10:173–180
11. Van Beek E, Pieterman E, Cohen L, Lowik C, Papapoulos S: Farnesyl pyrophosphate synthase is the molecular target of nitrogen-containing bisphosphonates. Biochem Biophys Res Commun 1999, 264: 108–111
12. Ylitalo R, Kalliovalkama J, Wu X, Kankaanranta H, Salenius JP, Sisto T, Lahteenmaki T, Ylitalo P, Porsti I: Accumulation of bisphosphonates in human artery and their effects on human and rat arterial function in vitro. Pharmacol Toxicol 1998, 83:125–131
13. Fournier P, Boissier S, Filleur S, Guglielmi J, Cabon F, Colombel M, Clezardin P: Bisphosphonates inhibit angiogenesis in vitro and testosterone-stimulated vascular regrowth in the ventral prostate in castrated rats. Cancer Res 2002, 62:6538–6544
14. Okamoto T, Yamagishi S, Inagaki Y, Amano S, Takeuchi M, Kikuchi S, Ohno S, Yoshimura A: Incadronate disodium inhibits advanced glycation end products-induced angiogenesis in vitro. Biochem Biophys Res Commun 2002, 297:419–424
15. Abid MR, Kachra Z, Spokes KC, Aird WC: NADPH oxidase activity is required for endothelial cell proliferation and migration. FEBS Lett 2000, 486:252–256
16. Babior BM: The NADPH oxidase of endothelial cells. IUBMB Life 2000, 50:267–269
17. Egami K, Murohara T, Shimada T, Sasaki K, Shintani S, Sugaya T, Ishii M, Akagi T, Ikeda H, Matsuishi T, Imaizumi T: Role of host angiotensin II type 1 receptor in tumor angiogenesis and growth. J Clin Invest 2003, 112:67–75
18. Torisu H, Ono M, Furue M, Ohmoto Y, Nakayama J, Nishioka Y, Sone S, Kuwano M: Macrophage infiltration correlates with tumor stage and angiogenesis in human malignant melanoma: possible involvement of TNFalpha and IL-1alpha. Int J Cancer 2000, 85:182–188
19. Abe R, Shimizu T, Shibaki A, Nakamura H, Watanabe H, Shimizu H: Toxic epidermal necrolysis and Stevens-Johnson syndrome are induced by soluble Fas ligand. Am J Pathol 2003, 162:1515–1520
20. Yamagishi S, Edelstein D, Du XL, Kaneda Y, Guzman M, Brownlee M: Leptin induces mitochondrial superoxide production and monocyte chemoattractant protein-1 expression in aortic endothelial cells by increasing fatty acid oxidation via protein kinase A. J Biol Chem 2001, 276:25096–25100
21. Miller FJ, Gutterman DD, Rios CD, Heistad DD, Davidson BL: Superoxide production in vascular smooth muscle contributes to oxidative stress and impaired relaxation in atherosclerosis. Circ Res 1998, 82:1298–1235
22. Miyazono K, Okabe T, Urabe A, Takaku F, Heldin CH: Purification and properties of an endothelial cell growth factor from human platelets. J Biol Chem 1987, 262:4098–4103
23. Yamagishi S, Yonekura H, Yamamoto Y, Katsuno K, Sato F, Mita I, Ooka H, Satozawa N, Kawakami T, Nomura M, Yamamoto H: Advanced glycation end products-driven angiogenesis in vitro. Induction of the growth and tube formation of human microvascular endothelial cells through autocrine vascular endothelial growth factor. J Biol Chem 1997, 272:8723–8730
24. Yamagishi S, Inagaki Y, Okamoto T, Amano S, Koga K, Takeuchi M, Makita Z: Advanced glycation end products-induced apoptosis and overexpression of vascular endothelial growth factor and monocyte chemoattractant protein-1 in human cultured mesangial cells. J Biol Chem 2002, 277:20309–20315
25. Nomura M, Yamagishi S, Harada S, Hayashi Y, Yamashima T, Yamashita J, Yamamoto H: Possible participation of autocrine and paracrine vascular endothelial growth factors in hypoxia-induced proliferation of endothelial cells and pericytes. J Biol Chem 1995, 270: 28316–28324
26. de Clerck LS, Bridts CH, Mertens AM, Moens MM, Stevens WJ: Use of fluorescent dyes in the determination of adherence of human leukocytes to endothelial cells and the effect of fluorochromes on cellular function. J Immunol Methods 1994, 172:115–124
27. Sasaki A, Kitamura K, Alcalde RE, Tanaka T, Suzuki A, Etoh Y, Matsumura T: Effect of a newly developed bisphosphonate, YM529, on osteolytic bone metastases in nude mice. Int J Cancer 1998, 77:279–285

28. Ueno T, Toi M, Saji H, Muta M, Bando H, Kuroi K, Koike M, Inadera H, Matsushima K: Significance of macrophage chemoattractant protein-1 in macrophage recruitment, angiogenesis, and survival in human breast cancer. Clin Cancer Res 2000, 6:3282–3289
29. Ohta M, Kitadai Y, Tanaka S, Yoshihara M, Yasui W, Mukaida N, Haruma K, Chayama K: Monocyte chemoattractant protein-1 expression correlates with macrophage infiltration and tumor vascularity in human esophageal squamous cell carcinomas. Int J Cancer 2002, 102:220–224
30. Salven P, Heikkila P, Joensuu H: Enhanced expression of vascular endothelial growth factor in metastatic melanoma. Br J Cancer 1997, 76:930–934
31. Ushio-Fukai M, Tang Y, Fukai T, Dikalov SI, Ma Y, Fujimoto M, Quinn MT, Pagano PJ, Johnson C, Alexander RW: Novel role of gp91phox-containing NAD(P)H oxidase in vascular endothelial growth factor-induced signaling and angiogenesis. Circ Res 2002, 91:1160–1167
32. Weis M, Heeschen C, Glassford AJ, Cooke JP: Statins have biphasic effects on angiogenesis. Circulation 2002, 105:739–745
33. Kim I, Moon SO, Kim SH, Kim HJ, Koh YS, Koh GY: Vascular endothelial growth factor expression of intercellular adhesion molecule 1 (ICAM-1), vascular cell adhesion molecule 1 (VCAM-1), and E-selectin through nuclear factor-kB activation in endothelial cells. J Biol Chem 2001, 276:7614–7620
34. Marumo T, Schini-Kerth VB, Busse R: Vascular endothelial growth factor activates nuclear factor-kappaB and induces monocyte chemoattractant protein-1 in bovine retinal endothelial cells. Diabetes 1999, 48:1131–1137
35. Zhang H, Yano S, Miki T, Goto H, Kanematsu T, Muguruma H, Uehara H, Sone S: A novel bisphosphonate minodronate (YM529) specially inhibits osteolytic bone metastases produced by human small-cell lung cancer cells in NK-cell depleted SCID mice. Clin Exp Metastasis 2003, 20:153–159
36. Yamno S, Zhang H, Hanibuchi M, Miki T, Goto H, Uehara H, Sone S: Combined therapy with a new bisphosphonate, minodronate (YM529), and chemotherapy for multiple organ metastases of small cell lung cancer cells in severe combined immunodeficient mice. Clin Cancer Res 2003, 9:5380–5385
37. Griendling KK, Sorescu D, Ushio-Fukai M: NAD(P)H oxidase: role in cardiovascular biology and disease. Circ Res 2000, 86:494–501
38. Lander HM, Tauras JM, Ogiste JS, Hori O, Moss RA, Schmidt AM: Activation of the receptor for advanced glycation end products triggers a p21(ras)-dependent mitogen-activated protein kinase pathway regulated by oxidant stress. J Biol Chem 1997, 272:17810–17814
39. Aikawa R, Komuro I, Yamazaki T, Zou Y, Kudoh S, Tanaka M, Shiojima I, Hiroi Y, Yazaki Y: Oxidative stress activates extracellular signal-regulated kinases through Src and Ras in cultured cardiac myocytes of neonatal rats. J Clin Invest 1997, 100:1813–1821
40. Irani K, Goldschmidt-Clermont PJ: Ras, superoxide and signal transduction. Biochem Pharmacol 1998, 55:1339–1346
41. van der Geer P, Hunter T, Lindberg RA: Receptor protein-tyrosine kinases and their signal transduction pathways. Annu Rev Cell Biol Chem 1994, 10:251–337
42. Meadows KN, Bryant PB, Pumiglia K: Vascular endothelial growth factor induction of the angiogenic phenotype requires Ras activation. J Biol Chem 2001, 276:49289–49298
43. Becker MD, Kruse FE, Azzam L, Nobiling R, Reichling J, Volcker HE: In vivo significance of ICAM-1-dependent leukocyte adhesion in early corneal angiogenesis. Invest Ophthalmol Vis Sci 1999, 40:612–618
44. Bingle L, Brown NJ, Lewis CE: The role of tumor-associated macrophages in tumor progression: implications for new anticancer therapies. J Pathol 2002, 196:254–265
45. Chin L, Tam A, Pomerantz J, Wong M, Holash J, Bardeesy N, Shen Q, O'Hagan R, Pantginis J, Zhou H, Horner II JW, Cordon-Cardo C, Yancopoulos GD, DePinho RA: Essential role for oncogenic Ras in tumor maintenance. Nature 1999, 400:468–472